

Field-Driven *Topological* Glass Transition in a Model Flux Line Lattice

Seungoh Ryu,¹ A. Kapitulnik,² and S. Doniach²

¹*Department of Physics, Ohio State University, Columbus, Ohio 43210*

²*Department of Applied Physics, Stanford University, Stanford, California 94305*

(Received 26 April 1996)

We show that the flux line lattice in a model layered high temperature superconductor becomes unstable above a critical magnetic field with respect to a plastic deformation via penetration of pairs of pointlike disclination defects. The instability is characterized by the competition between the elastic and the pinning energies and is essentially assisted by softening of the lattice induced by a dimensional crossover of the fluctuations as field increases. We propose that this mechanism provides a model of the low temperature field-driven disordering transition observed in neutron diffraction experiments on $\text{Bi}_2\text{Sr}_2\text{CaCu}_2\text{O}_8$ single crystals. [S0031-9007(96)01185-4]

PACS numbers: 74.60.Ec, 64.60.Cn, 74.60.Ge

The mixed state in the high temperature superconductors (HTSC) has been studied from a wide variety of perspectives over the past few years [1]. Among the interesting issues under debate are the question of how vortices freeze [2,3] in the so-called vortex glass phase [4] as well as the nature of the melted phase [5,6]. In particular, one expects an intricate interplay of the underlying layered nature of the host material and the random point pins in shaping the nature of the frozen phase.

A recent decoration performed on both sides of the $\text{Bi}_2\text{Sr}_2\text{CaCu}_2\text{O}_8$ single crystal suggests that vortex lines maintain their line integrity at least at very low field [7]. On the other hand, the rapid disappearance of Bragg peak intensity in the recent small angle neutron diffraction (SANS) [8] has been interpreted by the authors in terms of decomposition of lines into pancake vortices [9]. A Lindemann-like criterion is usually invoked in discussing such a “decoupling theory” [10], but it fails to explain how the transition is brought about, if there is one.

Traditionally the role of a pinning potential has been treated as a perturbation within the harmonic elastic framework. In the weak pinning limit, the perturbed lattice tries to optimize its free energy by forming elastic domains of correlated region with minimum elastic energy while it is fragmented in larger length scales to take advantage of the random potential energy [11]. Several attempts have been made recently to extend the simple dimensional argument [12] for length scales larger than the elastic volume, but without detailed considerations of topological defects. Their effect is expected to dominate for strong enough disorder, resulting in a dislocation dominated “glass phase” [13–15].

In an earlier paper [16] we showed that the dramatic features of the SANS results cannot be accounted for by a dimensional crossover alone of a “clean” lattice. We further suggested that the flux lattice in the highly anisotropic $\text{Bi}_2\text{Sr}_2\text{CaCu}_2\text{O}_8$ may suffer an instability against penetration of topological defects and therefore may deteriorate rapidly across a characteristic flux line density. More re-

cently, such a transition has been claimed to be observed also in a $\text{YBa}_2\text{Cu}_3\text{O}_{7-\delta}$ based superlattice [17]. In this Letter we report computer simulation studies of this transition using simulated annealing on a model flux line system. We start by noting that when the density of flux line in a layered HTSC is varied, the effective anisotropy of the lattice and the disorder strength change. As a result the elastic domains, described by an in-plane length R_d and an out-of-plane length L_d (defined later) may shrink. In particular, when L_d reaches the interlayer spacing, a new low temperature glass state that is dominated by disclinations appears. We propose that the transition to this phase is first order and is characterized by an explosive invasion of pointlike disclination pairs across a horizontal line in the B - T phase diagram.

Employing a vortex representation of the Lawrence-Doniach model [18], we consider a stack of coupled two dimensional vortex lattices with pancake vortex coordinates $\{r_{i,z}\}$ with i labeling the individual flux lines. An approximate pairwise interaction under periodic boundary conditions has been derived to make large scale numerical calculations possible [19]. With a choice of in-plane penetration depth $\lambda(0) = 1800 \text{ \AA}$, $d = 15 \text{ \AA}$, $\kappa = 100$, and anisotropy $\gamma = \sqrt{M_c/M_{qb}} = 55$, we obtain, for a clean system, a melting line $T_m(B)$ which is in reasonable agreement with the experimental result [14]. The random potential is modeled by potential wells of uniform depth U_p , of radius given by the lesser of $2\xi_{ab}$, and the grid size scattered at *random positions* of each layer with an areal density of $n_p = 1/a_p^2 \equiv B_p/\phi_0$. We choose $U_p = 5 \frac{d\phi_0^2}{8\pi^2\lambda^2(T)}$, $B_p = 150 \text{ G}$ for 64 lines in 16 (set #1) and 32 (set #3) layers which give the freezing temperature $\sim 40 \text{ K}$ for $1 < B < 20 \text{ kG}$ under a Lindemann-like criterion in reasonable agreement with the experimentally determined irreversibility line $T_{\text{irr}}(B)$. We also have results for a different pin density $B_p = 2.4 \text{ kG}$ in 16 layers (set #2). The line density ($\sim 100 \text{ G}$ – 2 kG) was varied by changing sizes of grid cells [19] and pin densities for

a fixed number of vortices. To obtain low temperature properties, we use a *simulated annealing* procedure starting at $T = 1.3T_f(B) \sim 50$ K and gradually decreasing T with steps of $dT = 5$ K over 40 000 Monte Carlo steps. At $T = 4$ K, an additional 20 000 steps were performed to measure physical quantities. This formally resembles a *field-cooling* procedure employed in typical measurements. The number of different pin configurations was limited to five for practical reasons. The disclination charge density $n_d(i, z)$ is measured every 50 steps through Delaunay triangulation [19] performed in each layer to determine the coordination number Z of each vortex. Then a charge of $q = (Z - 6)$ is assigned to $n_d(i, z)$. We also introduce an integer variable $n_d^*(i, z)$ which gives 1 for a disclination and 0 otherwise.

Results.—In the inset to Fig. 1 we show the partial Fourier transform $S(q_x, q_y, z = L)$ of the vortex density correlation function $\int d^2\rho \exp(iq\rho) \langle n_v(\rho, z = L) n_v(0, 0) \rangle$ as evaluated in our simulation where $n_v(\rho, z)$ is the local vortex density. Ideally, SANS with $q_z \sim 0$ aims to measure $\int dz S(q_x, q_y, z)$ and therefore for a macroscopic sample with $L \rightarrow \infty$, we expect it to be related to the diffraction pattern of [8]. The simulated Bragg peak intensities (dots in Fig. 1), decaying rapidly over a narrow range of $\delta B/B_{cz} \sim 0.3$, looks [20] strikingly similar to the appropriately scaled data from Cubitt *et al.* The values of B_{cz} were 1800 (set #1) and 550 (set #2) Gauss, while we used 500 G for the experimental

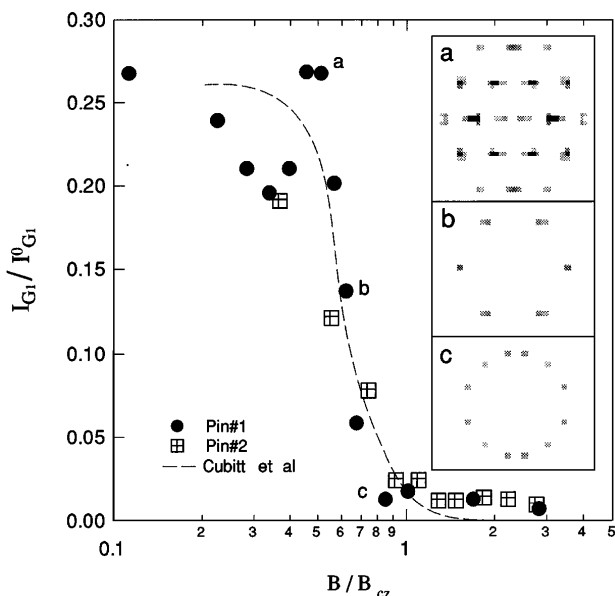


FIG. 1. The relative integrated intensity $I(G_1)/I^0(G_1)$ of the first order Bragg peak in the partial structure factor for set #1 and set #2. The intensity was normalized by that of the *clean* sample at the same temperature and field. The broken line is $I(G_1) \times G_1$ taken from the neutron scattering data [8] with the field scaled by a value at which the intensity reaches the flat bottom. The insets show the *simulated* diffraction pattern for three representative points [labeled (a), (b), (c)] of set #1 in the curve. Intensity for (c) was multiplied by a factor of 30.

data. The statistical deviation of the intensity $\delta I_{G1}/I_{G1}$ over five disorder configurations is within 20%. To verify what is driving the rapid drop, we look into the behavior of topological defects and the fraction of pinned vortices f_p which is given by $\langle \sum_{i,z} \Theta(r_{i,z}) \rangle / N$ where $\Theta(r)$ gives 1 if r is within any of the pinning wells and 0 otherwise. In Fig. 2 we observe a jump in f_p within the narrow range of $\delta B/B_{cz} \sim 0.2$, the same region over which the Bragg intensity vanishes. There is a corresponding increase in the total number of disclinations $\sum_{i,z} \langle |n_d(i, z)| \rangle$ accompanied by a rapid drop of the in-plane hexatic order parameter Ψ_6 [19]. It is interesting to note that we find the weak hexatic order is still present well into the high field phase and that their correlation along the c axis is sensitively dependent on the overall strength of the pins [21]. It disappears as field further increases, suggesting a possible sliver of a distinctive *hexatic* glass phase. We note that the kink observed in the pinned fraction around $B \sim 5B_{cz}$ could possibly signal the existence of an intermediate *hexatic* glass phase.

As shown in the inset to the low field side, a typical configuration has a finite number of defects, but they in general appear as neutral disclination pairs or quartets (equivalent to a bound pair of dislocations), healing each other over a finite length along the z axis. With these bound defects, the lattice order is disrupted only over a finite distance given by the size of these bound defects, and manifests itself as distinct Bragg spots of

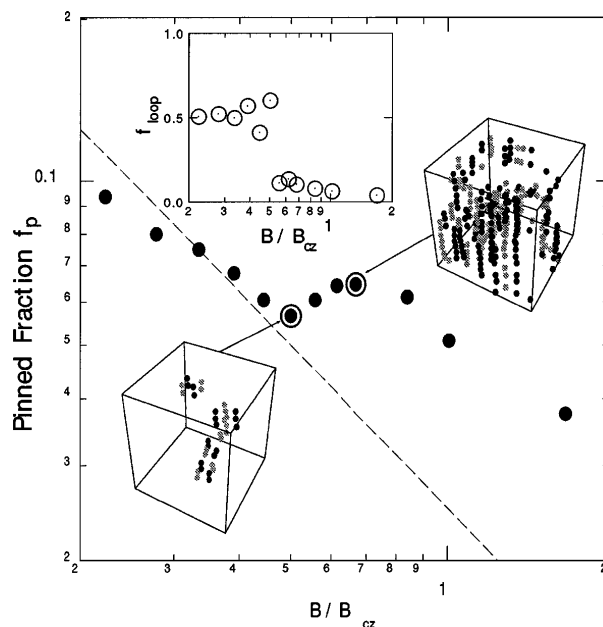


FIG. 2. Pinned fraction of vortices across the instability line for set #1. The broken line is a guide with $\sim B_p/B$. The abrupt increase in the pinned fraction is closely accompanied by the proliferation of topological defects as shown as black ($Z > 6$) and gray ($Z < 6$) dots in the insets. Also shown as an inset is the interlayer defect-density fluctuations f_{loop} (defined in the text).

Fig. 1. It is to be contrasted with the higher field configuration in which defects are threading *from top-to-bottom* layers of the sample in various sizes and separations. A convenient measure of relative frequency of defect loop termination inside our simulation box is given by measuring the interlayer defect density fluctuations $f_{\text{loop}} \equiv \langle 2|n_d^*(z) - n_d^*(z-1)| / (n_d^*(z) + n_d^*(z-1)) \rangle$ averaged over layers (inset of Fig. 2). The dramatic suppression of f_{loop} at high fields cannot be accounted for by an increase in n_d^* alone and is consistent with our observation that the phase is penetrated by unbound defect lines.

We define the probability distribution for length l of continuous defect lines: $\mathcal{P}(l) = [\langle \sum_{i,z} [1 - n_d^*(i,z)] [1 - n_d^*(i,z+l+1)] \prod_{z'=z+1}^{z+l} n_d^*(i,z') \rangle]$ where $\langle \dots \rangle$ means thermal and disorder averages. In a pin-free system, the distribution above $T_m(B)$ shows a gradual crossover behavior as B increases, reflecting the underlying dimensional crossover of the fluctuations of the lattice [14,22]. In this case of $T \ll T_f$ with quenched disorder, however, we observe a more dramatic change which suggests a field-driven phase transition. In Fig. 3 we show $\mathcal{P}(l)$ of continuous defect length l for fields $B/B_{cz} \approx 0.2-2$ averaged over five different pin configurations (set #1). Despite large statistical fluctuations at the large tail, we can clearly see that $\mathcal{P}(l)$ for high field $\sim e^{-\alpha l}$ qualitatively differs from the low field distribution for which $\mathcal{P}(l) = 0$ for $l > l_{\text{max}}(B)$. The exponential dependence for high field can easily be understood in terms of *pointlike* defects generated *independently in each layer* with a probability p . A probability for an accidentally aligned line of length l will then be $\mathcal{P}(l) \sim (1-p)^2 p^{l/d} \sim \exp[-\frac{l}{d} |\log p|]$. In the low field, the length of defect line is truncated by the defect energy outweighing the overall gain from random pins [23].

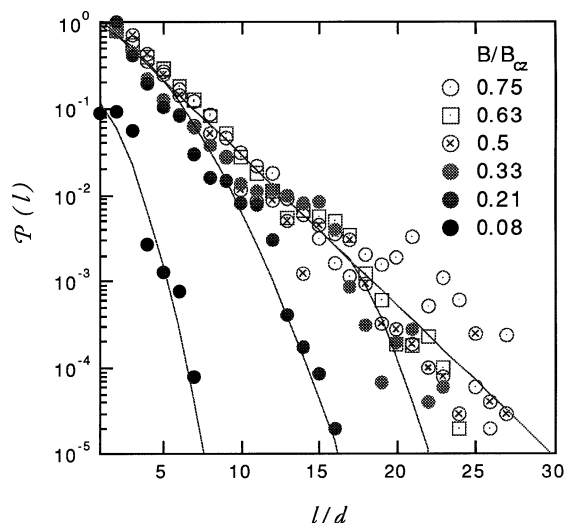


FIG. 3. $\mathcal{P}(l)$ for various values of B averaged over five different realizations of pins (set #3). The number of layers was 32. Filled circles correspond to the lattice phase while open symbols are for high field topological glass regime. Broken lines are guides for the eye.

This observation gives a clue in understanding the role of pins in the defect representation of the free energy. Clearly the pinning potential acts as an effective “temperature” to drive the topological defects into the lattice by encouraging vortices to make large excursions to seek optimal pinning configurations. The occurrence of these topological defects signals the breakdown of the elastic theory and the transition to a new defect-dominated phase. We can estimate the breakdown field B_{cz} as follows: Let us assume that the accumulated vortex displacements $u_i(x)$ reach $\mathcal{O}(a_B)$ over a volume V_d of radius R_d in the a - b plane, length L_d along the c axis. For $B < (U_p/\epsilon d)^4 B_p^2/B_J$, where $B_J \equiv \phi_0/(\gamma d)^2$, a variational minimization of elastic free energy yields $R_d/a_B < 1$, suggesting a breakdown of the 3D elastic approach. Note that $R_d/a_B \approx 1$ is a necessary but not sufficient condition for vanishing Bragg peaks since *bound* defect loops of finite sizes may occur in the lattice regime as shown in Fig. 3. Consequently we assume a very short ranged in-plane order and fix $R_d \sim \mathcal{O}(a_B)$, and perform a partial variational calculation for a tube of variable length $L_d|_{R_d \sim a_B}$ to obtain $L_d(B)/d \sim (\epsilon^2 d^2 B_J^2 / U_p^2 B_p B)^{1/3}$. The breakdown field B_{cz} is obtained from the condition $L_d(B_{cz}) < d$. Here we assume that the statistical gain in pinning energy by bending of such tubes is given by $U_p(n_p V_d/d)^{0.5+\delta}/a_B^2 L_d$ with $\delta = 0$, a rough approximation. Using the parameter values we chose, this yields $B_{cz} \sim 2.4$ kG (set #1), in reasonable agreement with the result of the simulation.

The results of the simulations may be summarized in a phase diagram given in Fig. 4. At low temperatures, the effective “noise temperature” of the random pinning field drives the system from a quasicrystalline phase at low fields to a defect-dominated topologically disordered phase at higher fields. This phase transition is facilitated by weak interlayer coupling, thus explaining the small value of the critical field B_{cz} for highly anisotropic materials such as $\text{Bi}_2\text{Sr}_2\text{CaCu}_2\text{O}_8$. On the other hand, for less anisotropic materials such as $\text{YBa}_2\text{Cu}_3\text{O}_{7-\delta}$, this instability should be pushed to a higher field. Because the disorder is induced by the pins, the vortices are still highly localized, hence in a glassy phase. We have not yet used our simulations to study the kinetics of this phase; however, from our previous studies [24] we expect the kinetics of the phase to be sub-Ohmic, so that it should still be a superconductor.

As the temperature is increased in the topologically disordered phase, we expect to reach a “depinning temperature” above which the defects become liquid-like and the transport would be Ohmic. The exact shape of the line of phase transitions between the quasicrystalline phase [25] and the topological glass phase depends on the details of the competing energies and may terminate at the melting line $T_m^{3D}(B)$, which was recently shown to bend toward and terminate at a field of ~ 500 G [26]. In the vicinity of

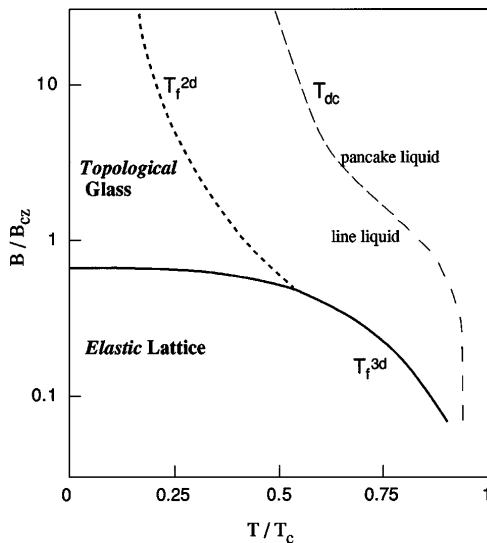


FIG. 4. Schematic phase diagram with *strong* point pins. The low field elastic lattice is turned into a topological glass state as B increases over B_{cz} . The freezing temperatures (T_f^{3d} and T_f^{2d}) are characterized by the dimensionality of topological defects as discussed in the text. We also note that there is a distinct decoupling crossover line T_{dc} in the liquid phase across which the vortex line segments disintegrate into pancake vortices by onset of cutting and reconnection [30].

the transition line B_{cz} , the explosion of topological defects will be expected to dominate the kinetics and may provide an explanation of the “fishtail” peak effect in the critical current observed as the B field is varied in this region of the phase diagram [27,28]. The results reported here are reminiscent of a transition observed independently by Gingras and Huse from simulations of a ferromagnetic 3D XY model with a random field [29].

The authors are grateful for the support by EPRI and the Air Force. S.R. was also supported by NSF Grant No. DMR94-02131, Midwest Superconductivity Consortium through DOE Grant No. DE-FG02-90ER-45427. S.R. acknowledges very useful discussions with Dr. Forgan and Dr. Stroud.

- [1] G. Blatter *et al.*, *Rev. Mod. Phys.* **66**, 1125 (1995).
- [2] C. A. Murray *et al.*, *Phys. Rev. Lett.* **64**, 2312 (1990).
- [3] E. M. Chudnovsky, *Phys. Rev. B* **40**, 11 355 (1989).
- [4] M. P. A. Fisher, *Phys. Rev. Lett.* **62**, 1415 (1989).
- [5] D. R. Nelson, *Phys. Rev. Lett.* **60**, 1973 (1988).
- [6] M. C. Marchetti and D. R. Nelson, *Phys. Rev. B* **42**, 9938 (1990).
- [7] Z. Yao *et al.*, *Nature (London)* **371**, 777 (1995).

- [8] R. Cubitt *et al.*, *Nature (London)* **365**, 407 (1993); see also E. M. Forgan *et al.*, *ibid.* **343**, 735 (1990).
- [9] J. R. Clem, *Phys. Rev. B* **43**, 7837 (1991).
- [10] A. Schilling *et al.*, *Phys. Rev. Lett.* **71**, 1899 (1993).
- [11] Y. Imry and S.-K. Ma, *Phys. Rev. Lett.* **35**, 1399 (1975); A. I. Larkin and Y. N. Ovchinnikov, *J. Low Temp. Phys.* **43**, 109 (1979).
- [12] J.-P. Bouchaud *et al.*, *Phys. Rev. B* **46**, 14 686 (1992); T. Nattermann, *Phys. Rev. Lett.* **64**, 2454 (1990); T. Giamarchi and P. L. Doussal, *ibid.* **72**, 1530 (1994).
- [13] D. A. Huse, *Physica (Amsterdam)* **197B**, 540 (1994).
- [14] Seungoh Ryu, Ph.D. thesis, Stanford University, 1994. See Chap. 10.
- [15] T. Giamarchi and P. Le Doussal, *Phys. Rev. B* **52**, 1242 (1995).
- [16] S. Ryu *et al.*, *Proc. SPIE Int. Soc. Opt. Eng.* **2157**, 12 (1994).
- [17] H. Obara *et al.*, *Phys. Rev. Lett.* **74**, 3041 (1995).
- [18] W. E. Lawrence and S. Doniach, in *Proceedings of LT12, Kyoto, Japan*, edited by E. Kanda (Keigaku, Tokyo, 1971), p. 361.
- [19] S. Ryu *et al.*, *Phys. Rev. Lett.* **68**, 710 (1992).
- [20] Because of screening of the field, the Bragg peak intensity $I_0(G_1)$ for a clean lattice is expected to behave as $\sim 1/\sqrt{B}$ [8,16]. We emphasize the existence of a phase transition by factoring this dependence out as shown in Fig. 1 of $I(G_1)/I_0(G_1)$, while SANS data shows $I(G_1)$.
- [21] For $B_p = 150$ G we have $|\Psi_6|^2 \sim 0.2$ with $\langle \Psi_6(z)\Psi_6(z-1)^* \rangle \sim 0.2$, while for $B_p = 2.4$ kG they were 0.1 and 0.01 at the field where the Bragg peak intensity vanishes. Both Ψ_6 and its interlayer correlation monotonically decreases as field further increases.
- [22] Seungoh Ryu and D. Stroud, *Phys. Rev. B* **54**, 1320 (1996).
- [23] There appears to be a “confinement” phenomenon due to the long ranged in-plane attraction of disclinations (dislocations) of opposite charge (Burger’s vectors). This restricts the defect loops to finite sizes in the low field region, while at high fields the defects may be viewed as dense, infinite loops meandering across layers and colliding with each other.
- [24] Seungoh Ryu *et al.*, *Phys. Rev. Lett.* **71**, 4245 (1993).
- [25] In the case of a defect free model with weak disorder, existence of a similar lattice phase has been predicted and termed *Bragg glass* in [15]. Our result suggests that the lattice order also survives the appearance of *bound defects*.
- [26] E. Zeldov *et al.*, *Nature (London)* **375**, 373 (1995).
- [27] Y. Yeshurun *et al.*, *Phys. Rev. B* **49**, 1548 (1994).
- [28] K. A. Moler *et al.* (to be published).
- [29] M. J. P. Gingras and D. A. Huse, *Phys. Rev. B* **53**, 15 193 (1996).
- [30] M. C. Hellerqvist *et al.*, *Physica (Amsterdam)* **230C**, 170 (1994).